Journal of Hydrology (NZ) 49 (2): 61-68 2010

Continuous monitoring of water discharge, temperature, and salinity in a tidal spillway using fluvial acoustic tomography

Kiyosi Kawanisi,[1] Mohn Razaz,[1] Gregory S. DeCosta[2] and Chamika De Costa[3]

[1] *River and Coastal Engineering Laboratory, Department of Civil and Environmental Engineering, Hiroshima University, Higashi Hiroshima, Japan.*

[2] *Department of Engineering and Construction, Open Polytechnic of New Zealand, Lower Hutt, Wellington, New Zealand.*
Corresponding author: Gregory.DeCosta@openpolytechnic.ac.nz

[3] *Department of Civil Engineering, University of Auckland, Auckland, New Zealand.*

Abstract

Data on river discharge is an important hydrological factor for river and coastal planning and management, control of water resources, and environment conservation. However, it is difficult to measure cross-sectional mean water velocity in complex flows such as tidal estuaries or during extreme hydrologic events such as floods. In this study, water discharge in a shallow tidal channel had been continuously measured using a new fluvial acoustic tomography system. In addition to measuring water discharge, mean water temperature and salinity were deduced from processing the sound speed data collected by the fluvial acoustic tomography system. The system was installed at a shallow tidal channel where water depth and salinity change significantly. It was found that the acoustic tomography system could successfully measure the cross-sectional mean velocity over a long duration.

Introduction

It has been recognized that reliability and safety are two pressing issues in collecting and evaluating river discharge data. For continuous measurement of water discharge, different equipment is available, such as acoustic velocity meters and horizontal acoustic Doppler current profilers (Catherine and DeRose, 2004; Wang and Huang, 2005). The main drawback of these methods is that often the number of velocity sample points in the cross-section of stream is not sufficient to estimate cross-sectional mean velocity.

Although several methods have been introduced to estimate the velocity distribution (e.g., by Chiu and Hsu, 2006 or Chiu *et al.*, 2005; Maghrebi, 2006), the results are disputable in complex flow field such as stratified tidal flows. Thus, innovative methods or equipment are required for continuous measurement of water discharge in tidal estuaries.

In this study, a fluvial acoustic tomography system is developed and utilized to measure the cross-sectional mean velocities in the Ota River diversion channel, which has large changes in water depth, as well as in salinity. The fluvial acoustic tomography system has advantages over competing techniques, namely accurate measurement of travel time using a GPS clock, and a high signal-to-noise ratio due to modulation by random M-sequence (Kawanisi *et al.*, 2010).

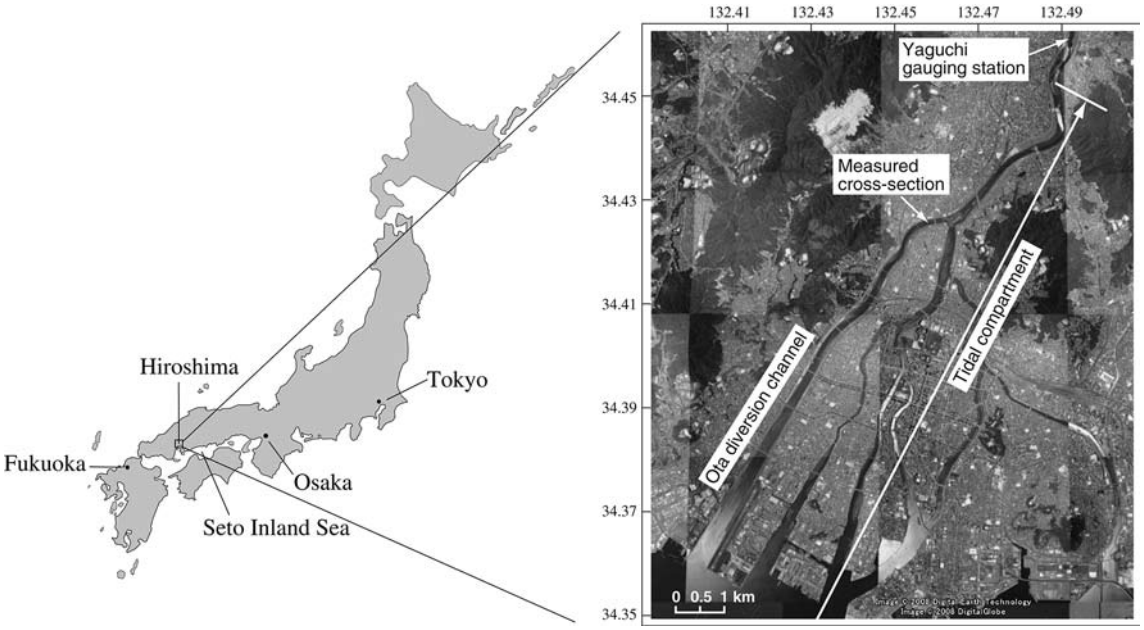

Figure 1 – Study area and observation site.

Study area and method

The Ota River bifurcates into two main branches at about 9 km upstream from the river mouth (Fig. 1). The upstream limit of tidal influence of the Ota River estuary is about 13 km upstream from the mouth. The tidal range of an extreme spring tide at the mouth is about 4 m.

Freshwater runoff is usually curtailed by the Gion sluice gates, which are located at the bifurcation point. Usually only one sluice gate is slightly opened. The cross-sectional area of the stream is 32 m × 0.3 m up to the level of flow spillover. During floods all sluice gates are completely open and the freshwater runoff from the Gion sluice rises to about half of the river's discharge. The Ota river discharge is estimated by rating curves at Yaguchi gauging station, which is located 14 km upstream from the mouth.

The observation site was located 246 m downstream from the Gion sluice gates (Fig. 1). The Ota diversion channel at the site is 120 m wide and the water depth ranges from 0.3 m to 3 m due to the tide. The salt water in the Ota River can intrude to about 11 km upstream from the mouth.

Several broad-band Omni-directional transducers were installed diagonally across the channel, as shown in Figure 2. The transducers (ITC3422) were manufactured by ITC, and their central frequency was 30 KHz. The angle between sound pass and stream direction θ was 30 degrees. The transducers were mounted at a height of 0.2 m above the bottom. The sound pulses of the acoustic tomography system were simultaneously transmitted from the omni-directional transducers every minute, triggered by a GPS clock. The acoustic wave is a linear wave, hence there is no potential interference from multiple paths.

Three moored acoustic Doppler current profilers (ADCPs) were used to validate the velocity data of the fluvial acoustic tomography system. Three ADCPs arranged

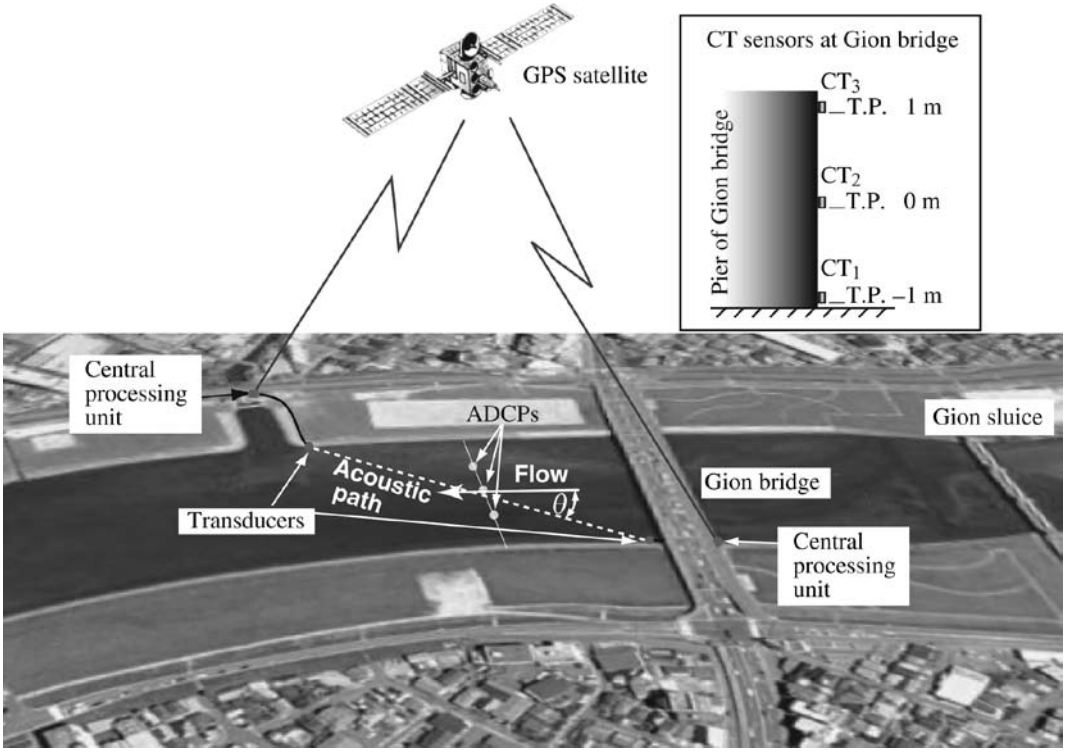

Figure 2 – Schematic diagram of the method of measurement.

along the Gion Sluices in a way that two ADCPs were 30 m apart from each other while the central ADCP location was aligned with the river centerline. The distance between the array of ADCPs (transverse line) and the Gion Bridge was 70 m.

The vertical distribution of water temperature and salinity were measured every 10 minutes by Conductivity and Temperature (CT) sensors attached to the pier of the Gion Bridge, 40 m from the left bank (Fig. 2). In addition, the cross-sectional distribution of temperature and salinity were measured by a Conductivity, Temperature, Depth (CTD) instrument cast from the Gion Bridge. Transverse spacing of the CTD casts was 20 m and crossing time was about 10 minutes. The CTD observations were carried out from 12:20 PM on the 3rd July to 9:50 AM on the 4th of July. It was noted that continuous data measured by CT sensors had a regular cycle synchronous with the tide. Thus, the CTD observations probably capture the variability of salinity and temperature distribution caused by the tide.

Measurement principles

The applied basic principle is similar to that used in an acoustic velocity meter, in other words the cross-sectional mean velocity is calculated using the "time of travel method" (Sloat and Gain, 1995). The fluvial acoustic tomography system is able to estimate cross-sectional mean velocity using sound paths that cover the section. In order to estimate the cross-sectional mean velocity, the sound paths have to pass all layers between the bottom and the water surface. If the sound speed has an inhomogeneous distribution in the water, then the curve that is produced or

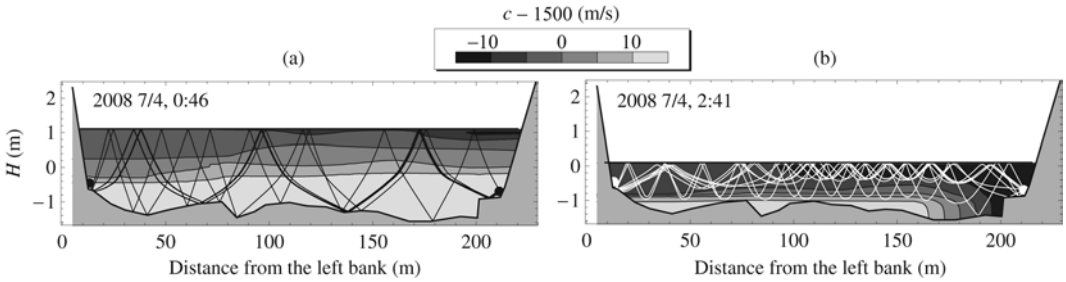

Figure 3 – Distribution of sound speed and results of ray simulation.

drawn by the rays follows Snell's law of refraction. In this paper, ray simulations were obtained and implemented by solving the following differential equations (Dushaw and Colosi, 1998):

$$\frac{d\varphi}{dr} = \frac{\partial c}{\partial r}\frac{1}{c}\tan\varphi - \frac{\partial c}{\partial z}\frac{1}{c} \qquad (1)$$

$$\frac{dz}{dr} = \tan\varphi$$

$$\frac{dt}{dr} = \frac{\sec\varphi}{c}$$

where φ is angle of the ray to the horizontal axis r, z is vertical coordinate, and t is the time. Here, the sound speed c was estimated by Medwin's formula (Equation (2)) as a function of temperature T (°C), salinity S, and depth D (m) (Medwin, 1975). This has been done within the following ranges: i.e., $0 \le T \le 35$°C, $0 \le S \le 45$, and $0 \le D \le 1\,000$ m:

$$c = 1\,449.2 + 4.6T - 0.055T^2 + 2.9\times10^{-4}T^3 + (1.34 - 0.01T)(S - 35) + 0.016D \qquad (2)$$

Figure 3 shows typical examples of distributions of the sound speed and results of the ray simulation just after high water during spring tide (HWS) and just before low water during spring tide (LWS). The sound speed was calculated from projected data of the CTD cast from the Gion Bridge. From this distribution it could be seen that salinity increases with depth. Sound speeds ranged from 1515 m/s in deeper layers to 1485 m/s near the surface. The carrier wave of 30kHz is considered as a linear wave, hence there is no potential interference in the carrier wave. However the multi-paths which are face-modulated by the M-sequence have potential interferences. The interferences broaden the cross-correlation between received signal and M-sequence. As a result a small error can be generated for the travel time measurement. Unfortunately the error is difficult to estimate in practice.

The projections of the CTD sensor data on the cross-section along the ray paths may include some error. Long-term CTD measurements on the cross-section along the transmission line are difficult. We assume that the projections do not widely alter the results of ray patterns. Most of the time, the sound paths cover the cross-section (as shown in Figure 3a). Unfortunately, sometimes an established salt wedge near the bed, which may be detected by the CTD sensors and the array of CT sensors attached to the pier of the Gion Bridge, causes the sound paths to be reflected; consequently, some of the sound paths are unable to penetrate into the lower layers, (see Figure 3b, which depicts a typical condition under strong stratification). In this case, the cross-sectional mean velocity is somewhat overestimated by the acoustic tomography system. Therefore the cross-sectional mean velocity should be modified using the velocity

distribution of two-layer flow when there is a salt wedge under the transducer (Kawanisi *et al.*, 2010).

The channel bathymetry along the transmission line was surveyed (with an accuracy of 0.01 m) on 17th March 2008, 16th June 2009 and 21st August 2009. The changes in channel bathymetry were small. As a result, the changes hardly affect the cross-sectional area.

The relative error of mean velocity along the sound path is estimated by Equation (3), (Kawanisi *et al.*, 2010).

$$\frac{\delta u_m}{u_m} = \frac{\delta L}{L} - 2\frac{\delta t_m}{t_m} + \frac{\delta(\Delta t_m)}{\Delta t} \approx \frac{\delta L}{L} + \frac{\delta(\Delta t_m)}{\Delta t} \quad (3)$$

Therefore, the error of mean velocity δu_m is expressed as:

$$\delta u_m = \frac{\delta L}{L} u_m + \frac{c_m^2}{2L}\delta(\Delta t) \quad (4)$$

The sound path length is estimated from the results of the ray simulations using Equation (5).

$$L = \int_a^b \sqrt{1 + (dz/dr)^2}\, dx \quad (5)$$

The amplitude of the fluctuations of L caused by the tides was about 0.1 m. Thus, $\frac{\delta L}{L}$ is negligible for the mean velocity. In general, the fluctuations of L are negligible for the velocity error because the ratios of depth and width are small in rivers. However, the term $\frac{c_m^2}{2L}\delta(\Delta t)$ on the right-hand side of Equation (4) can be neglected if $\delta(\Delta t)$ is very small because the mean sound speed c_m is very large. In the case of $\delta(\Delta t)=5\times10^{-7}$s (GPS clock accuracy) and L = 2000 m,

$$\delta u_m \approx \pm 0.0025 u_m \pm 3\text{mm/s} \quad (6)$$

Since the errors of conventional electronic clocks are unduly large, it is not possible to measure the precise velocity with the conventional clocks.

Results and discussions

Comparison between the fluvial acoustic tomography system and acoustic Doppler current profilers

Figure 4 shows temporal variations of the cross-sectional mean velocity v_m and the water level H. The thick gray line denotes the cross-sectional mean velocity deduced from three moored ADCPs. The broken line denotes the water level. Unfortunately, we are unable to discuss the accuracy of the fluvial acoustic tomography system using the results from the ADCPs because the accuracy of velocity data from three ADCPs is low; the strong non-uniformity of flow at the observation site means more ADCPs are needed. However, it is found that the difference between velocities acquired by the acoustic tomography system and the ADCPs is small (Fig. 4). Thus, we can conclude that the cross-sectional mean velocity obtained from the fluvial acoustic tomography system

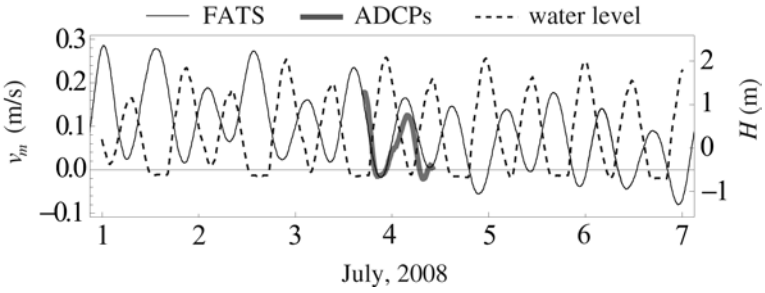

Figure 4 – Comparison of cross-sectional mean velocity between the fluvial acoustic tomography system (FATS) and acoustic Doppler current profilers (ADCPs).

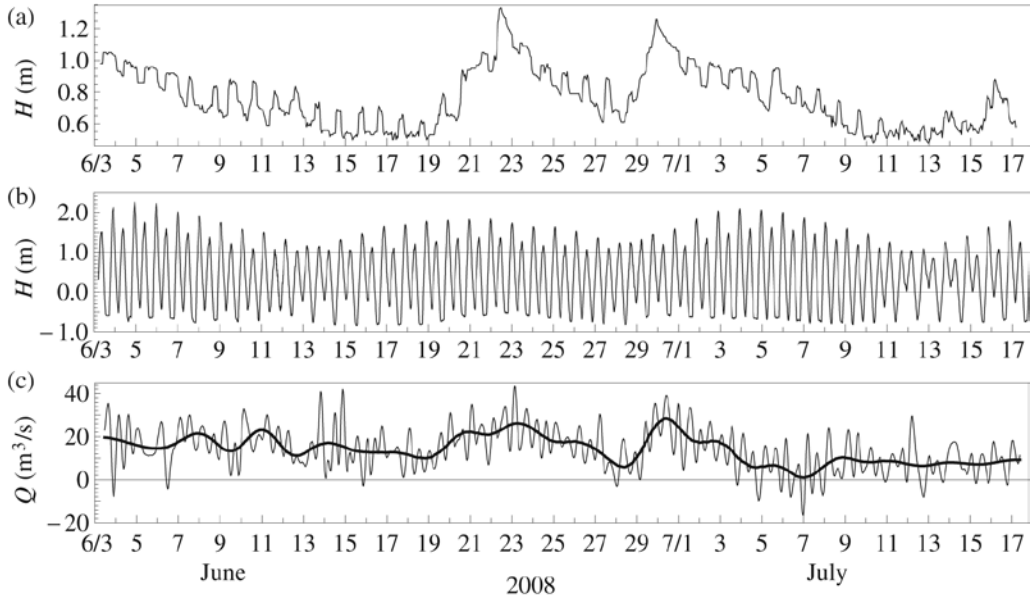

Figure 5 – Temporal variations of (a) water level at Yaguchi, (b) water level at Gion and (c) water discharge for 44 days.

shows acceptable compliance with the results derived from the ADCPs.

Temporal variation of water discharge

The water discharge was calculated by the acoustic tomography system from:

$$Q = A(H)v_m \sin\theta = A(H)u_m \tan\theta \qquad (7)$$

where A is the cross-sectional area in which sound paths travel, u_m is the mean velocity along the sound paths, and θ is the angle between sound path and streamline.

Temporal variations of the water levels at Yaguchi and Gion, and flow discharge are illustrated in Figure 5 for 44 days. As can be seen, limiting the runoff from the Gion Gates led to dominance of tidal effects. Long-duration measurement of the discharge was carried out successfully. Thus, employing fluvial acoustic tomography is a promising method for continuous measurement of the discharge. The values modified using the velocity distribution of two-layer flow were on average about 10% smaller than values without correction for the observation period. The trend of discharge in Figure 5 corresponds with the change of water level at the Yaguchi gauging station.

Temporal variation of the mean sound speed, water temperature and salinity

Temporal variations of the cross-sectional mean sound-speed of the fluvial acoustic tomography system and depth-mean water temperatures T_G measured by the CT sensors attached to the Gion Bridge pier are plotted in Figure 6. It is found that the trend of the sound speed c is similar to that of water temperature. The variations of c are caused by salinity fluctuations. Equation (1) suggests that c is more sensitive to water temperature than salinity. Hence, we can deduce the trend of water temperature $\overline{T}_{FAT}$ from c if it is assumed that the effect of salinity changes is negligible. Figure 7 shows the relation between $\overline{T}_{FAT}$ and $\overline{T}_G$. The correlation between $\overline{T}_{FAT}$ and $\overline{T}_G$ is high.

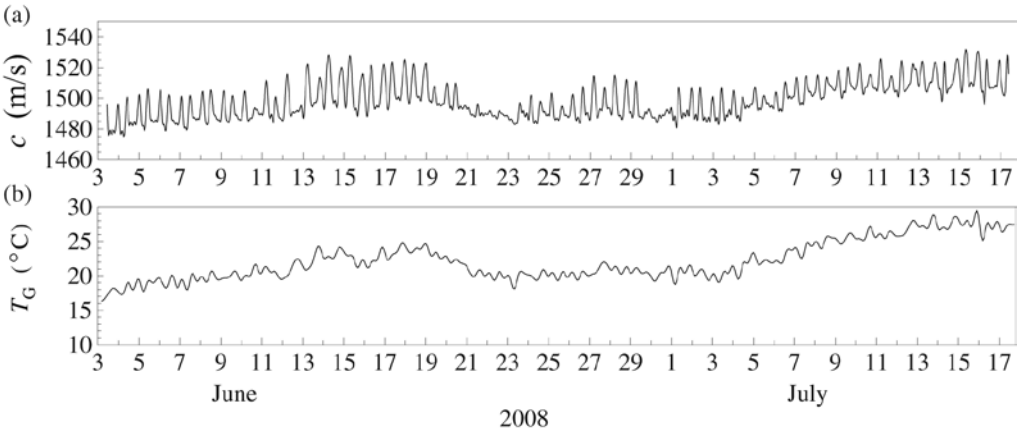

Figure 6 – Temporal variations of (a) cross-sectional mean sound speed, (b) water temperature at the depth of mean temperature at Gion Bridge for 44 days.

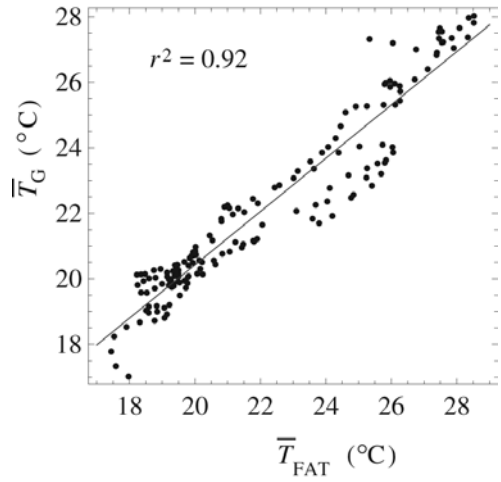

Figure 7 – Relation between the trends of water temperature deduced from fluvial acoustic tomography and the CT sensors at Gion Bridge.

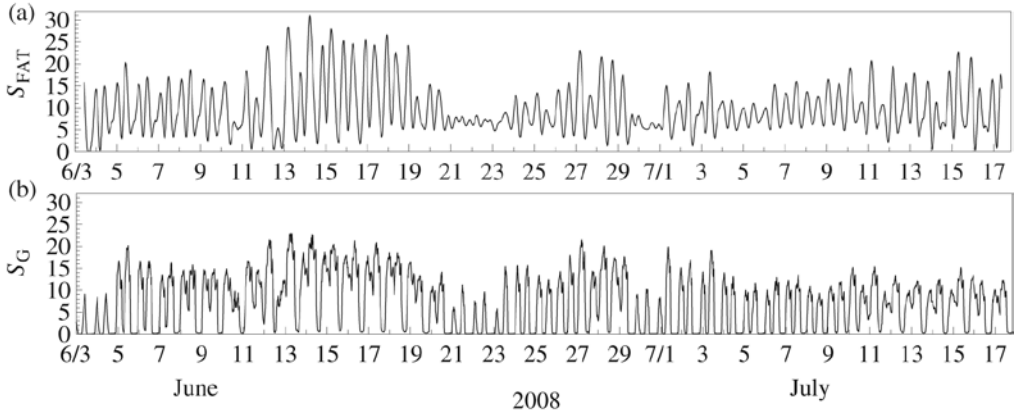

Figure 8 – Temporal variations of (a) cross-sectional mean salinity and (b) depth mean salinity at Gion Bridge for 44 days.

Temporal variation of the cross-sectional mean salinity S_{FAT} deduced from c and T_G is plotted in Figure 8 together with depth-mean water temperature S_G measured by the CT sensors. Large tidal fluctuations of salinity are found in Figure 8. It is possible that because sampling was carried out at two different locations, S_{FAT} and S_G are not identical, i.e., the sampling section of the fluvial acoustic tomography system was placed downstream of the CT sensors (the location of the transducer at the right bank is 174 m downstream from the Gion Bridge). Peaks of salinity decrease during higher discharges of the Ota River (see Figure 5a).

Conclusions

A fluvial acoustic tomography system that utilizes a GPS clock and M-sequence modulation was developed and applied to a shallow tidal river with a complex flow field. The acoustic tomography system, consisting of several transducers that were installed diagonally across the channel, was able to measure the cross-sectional mean velocity. A sufficiently high signal-to-noise ratio was obtained owing to the 10th-order M-sequence modulation. Thus, we believe that fluvial acoustic tomography works well, even throughout floods in which turbidity and sound noise are very high.

In addition to the measurement of water discharge, the water temperature and salinity were deduced from the mean sound speed measured by fluvial acoustic tomography. This means that freshwater discharges can be estimated more precisely using the fluvial acoustic tomography system than by existing velocimeters such as acoustic velocity meters and acoustic Doppler current profilers with salinity sensors.

References

Catherine, A.R.; DeRose, J.B. 2004: Investigation of hydro acoustic flow-monitoring alternatives at the Sacramento river at Freeport, California: Results of the 2002-2004 pilot study. Scientific Investigation Report, USGS (2004-5172).

Chiu, C.-L.; Hsu, S.-M.; Tung, N.-C. 2005: Measuring real-time stream flow using emerging technologies: Rader, hydro acoustics, and the probability concept. *Journal of Hydrology 357*: 1-10.

Chiu, C.-L.; Hsu, S.-M. 2006: Probabilistic approach to modeling of velocity distributions in fluid flows. *Journal of Hydrology 316*: 28-42.

Dushaw, B.D.; Colosi, J.A. 1998: Ray tracing for ocean acoustic tomography. Technical Memorandum, Applied Physics Laboratory, University of Washington, (TM 3-98), 31.

Kawanisi, K.; Razaz, M.; Kaneko, A.; Watanabe, S. 2010: Long-term measurement of stream flow and salinity in a tidal river by the use of the fluvial acoustic tomography system. *Journal of Hydrology 380(1-2)*: 74-81. [doi: 10.1016/j.jhydrol.2009.10.024]

Maghrebi, M.F. 2006: Application of the single point measurement in discharge estimation. *Advances in Water Resources 29(10)*: 1504-1514.

Medwin, H. 1975: Speed of sound in water: A simple equation for realistic parameters. *Journal of the Acoustical Society of America 58*: 1318.

Sloat, J.V.; Gain, W.S. 1995: Application of acoustic velocity meters for gauging discharge of three low-velocity tidal streams in the St. John River Basin, Northeast Florida. U.S. Geological Survey, Water-Resources Investigations Report, 95-4230, 26 p.

Wang, F.; Huang, H. 2005: Horizontal acoustic Doppler current profiler (H-ADCP) for real-time open channel flow measurement: flow calculation model and field validation. In: *XXXI IAHR CONGRESS*, Seoul, Korea, 319-328.

Manuscript received 16 September 2009; accepted for publication 3 August 2010